Electrical conduction mechanisms in natively doped ZnO nanowires (II)



2010 Nanotechnology 21 145202

(http://iopscience.iop.org/0957-4484/21/14/145202)

Nanotechnology **21** (2010) 145202 (5pp) doi:10.1088/0957-4484/21/14/145202

# Electrical conduction mechanisms in natively doped ZnO nanowires (II)

**Lin-Tzung Tsai**[1], **Shao-Pin Chiu**[1], **Jia Grace Lu**[2] **and Juhn-Jong Lin**[1,3]

[1] Institute of Physics, National Chiao Tung University, Hsinchu 30010, Taiwan
[2] Department of Physics and Astronomy, University of Southern California, Los Angeles, CA 90089, USA
[3] Department of Electrophysics, National Chiao Tung University, Hsinchu 30010, Taiwan

E-mail: jjlin@mail.nctu.edu.tw

Received 8 December 2009, in final form 10 February 2010
Published 10 March 2010
Online at stacks.iop.org/Nano/21/145202

**Abstract**

We have measured the intrinsic electrical resistivities, $\rho(T)$, of three individual single-crystalline ZnO nanowires (NWs) from 320 down to 1.3 K. The NWs were synthesized via carbon thermal chemical vapor deposition and the four-probe Pt contacting electrodes were made by the focused-ion-beam technique. Analysis of the overall temperature behavior of $\rho(T)$ confirms that the charge transport processes in natively doped ZnO NWs are due to a combination of the thermal activation conduction and the nearest-neighbor hopping conduction processes, as proposed and explained in a recent work (Chiu *et al* 2009 *Nanotechnology* **20** 015203) where the ZnO NWs were grown by a different thermal evaporation method and the four-probe electrodes were made by the electron-beam lithography technique. Taken together, the observations of these two complementary studies firmly establish that the electrical conduction mechanisms in natively doped ZnO NWs are unique and now satisfactorily understood.

(Some figures in this article are in colour only in the electronic version)

## 1. Introduction

Owing to the potential applications in the emerging nanoelectronics and optoelectronics, zinc oxide (ZnO) has recently attracted intense theoretical and experimental attention [1, 2]. ZnO is a wide bandgap semiconductor and is a native n-type material. The n-type characteristics of electronic conduction in nominally undoped ZnO materials originate from the native defects such as structural imperfections and unintentional impurities (in particular, hydrogen atoms) [3]. Among the various physical (optical, electrical, mechanical, piezoelectric, etc) properties, the electrical properties in ZnO are 'complex' and often thought to be intangible. The situation becomes even more uncertain in the cases involving quasi-one-dimensional ZnO nanowire (NW) materials and devices. This widespread (mis)conception largely arises from the fact that the electrical transport properties measured by different groups often differ significantly. For instance, the reported room temperature resistivities can differ by as many as several orders of magnitude [4]. Also, the measured temperature behaviors of resistance are very different. As a consequence, various conduction mechanisms, including the thermal activation conduction [5, 6], the Mott variable-range-hopping (VRH) conduction [7, 8] and the Efros–Shklovskii VRH conduction [9, 10] processes, have been proposed to explain the data obtained in different experiments. In our opinion, such discrepancies in the explanation may be ascribed to the fact that most previous measurements had been performed with either the two-probe method [6, 10] or a field-effect transistor (FET) configuration [8], where the contact resistance could be very large and depend strongly on the temperature. Therefore, the measured resistance and the temperature behavior do not reflect the intrinsic resistance of the NW sample under study, and hence making it impossible (or, sometimes, misleading) to draw a reliable physical picture for the microscopic conduction processes.

In a recent study of the electrical transport properties in individual ZnO NWs by Chiu *et al* [11] (hereafter denoted as (I)), some of us had carried out careful and systematic four-probe measurements on individual NWs over

 

**Table 1.** Values of measured ($d$ and $\rho(300\ \mathrm{K})$) and least-squares-fitted ($\rho_i$s, $\rho_0$ and $E_i$s) parameters for three single-crystalline, natively doped ZnO NWs. $d$ is diameter. $\rho_i$ ($i = 1, 2, 3$), $E_i$ and $\rho_0$ are defined in equation (1). Owing to uncertainties in the NW and electrode dimensions, the absolute values of $\rho(300\ \mathrm{K})$ are accurate to ≈15%. The fitted values of $\rho_1$, $\rho_2$ and $\rho_3$ are subject to uncertainties of ≈2%, 3% and 5%, respectively.

| NW | $d$ (nm) | $\rho(300\ \mathrm{K})$ (Ω cm) | $\rho_1$ (Ω cm) | $E_1$ (meV) | $\rho_2$ (Ω cm) | $E_2$ (meV) | $\rho_3$ (Ω cm) | $E_3$ (meV) | $\rho_0$ (Ω cm) |
|---|---|---|---|---|---|---|---|---|---|
| Z-1 | $60 \pm 3$ | 0.031 | 0.090 | $26.1 \pm 0.3$ | 0.11 | $2.23 \pm 0.10$ | 0.21 | ≃0.000 17 | 0.067 |
| Z-1[a] | $60 \pm 3$ | 0.031 | 0.091 | $26.0 \pm 0.3$ | 0.11 | $2.23 \pm 0.01$ | — | — | 0.051 |
| Z-2 | $105 \pm 5$ | 0.037 | 0.072 | $22.8 \pm 0.7$ | 0.11 | $2.34 \pm 0.12$ | 0.13 | $0.77 \pm 0.03$ | 0.184 |
| Z-3 | $95 \pm 5$ | 0.047 | 0.031 | $26.3 \pm 0.7$ | 0.12 | $4.47 \pm 0.19$ | 0.48 | $0.83 \pm 0.02$ | 1.78 |

[a] In this case, the $\rho_3$ ($E_3$) term was ignored by setting $\rho_3^{-1} = 0$ in the least-squares fits of equation (1) with the measured $\rho(T)$.

a wide range of temperatures from 300 down to 0.25 K. The measurements allowed the authors to propose, for the first time, a satisfactory explanation for the charge transport mechanisms in natively doped ZnO NWs. In particular, the authors explained that the charge conduction processes are due to a combination of the thermal activation conduction and the nearest-neighbor hopping (NNH) conduction processes. The underlying electronic band structure which facilitated such unique conduction processes is due to a splitting of the impurity band into a lower D band and an upper $D^-$ band (see figure 3 of (I)) [9, 11]. The splitting of the impurity band originated from the intricate materials properties of as-grown ZnO NWs, i.e. a moderately high n-type doping accompanied with a slight self-compensation, which are essentially independent of the NW growth methods. (It is known that most ZnO NWs reported in the literature possess electron concentrations of the order of $\sim 5 \times 10^{16}$–$10^{18}\ \mathrm{cm}^{-3}$ [11].)

This meaningful interpretation for the electrical conduction mechanisms in ZnO NWs undoubtedly deserves a further cross-check. Therefore, in the present work, we have measured the *intrinsic* resistivities, $\rho(T)$, in three individual ZnO NWs from 320 down to 1.3 K and analyzed their overall temperature behavior. The NWs were synthesized via carbon thermal chemical vapor deposition and the four-probe electrodes were made by the focused-ion-beam (FIB) technique while, in (I), the NWs were obtained from a different source and grown by a different thermal evaporation method [12]. Besides, there the submicron electrodes were made by the electron-beam lithography technique. Employing both a distinct NW growth method and a different electrode contacting technique in this work allow us to perform a stringent and convincing test of the interpretation for the intrinsic resistivities in ZnO NWs proposed in (I). Our new results, which are in good accord with the observations of (I), are reported below.

## 2. Experimental method

ZnO NWs were synthesized via carbon thermal chemical vapor deposition. The growth characteristics and atomic structure had been presented previously [13]. In this work, we concentrate on three NWs with diameters of 60–105 nm and lengths of a few microns for electrical transport studies. The relevant parameters for our NWs are listed in table 1.

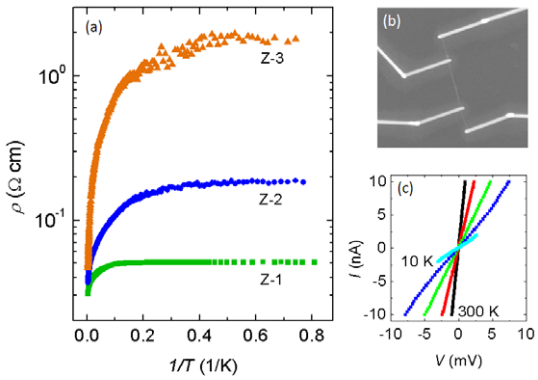


**Figure 1.** (a) Variation of logarithm of resistivity with reciprocal temperature for three ZnO NWs between 1.3 and 320 K. Notice that the resistivity approaches a constant at the lowest measurement temperatures in every NW. (b) An SEM image for the four-probe Z-1 NW device fabricated with the FIB technique. The sample length between the two (inner) voltage probes is 3.9 $\mu$m. (c) The current–voltage curves for the Z-3 NW at 10, 20, 40, 100 and 300 K.

To fabricate individual NW devices for four-probe electrical transport measurements, we first made micron-sized Ti/Au (10/60 nm) pads on an Si substrate which was capped with a 300 nm thick $SiO_2$ layer. ZnO NWs were then dispersed on the $SiO_2$-capped Si substrate. Individual ZnO NWs were identified and electrically connected to the micron-sized pads by utilizing the standard FIB technique. In an FEI Dual-Beam NOVA 200 FIB instrument, we applied the $Ga^+$-beam-induced deposition method with a methyl cyclopentadienyl trimethyl platinum $(CH_3)_3Pt(C_pCH_3)$ injector to selectively deposit Pt metal for connecting the ZnO NWs with the Ti/Au pads. The $Ga^+$ ions were accelerated to 30 kV at 10 pA and injected into the NWs during the Pt deposition. The dimensions of the Pt contacting electrodes were set 80 nm in width and 100 nm in thickness, but the actual width was 300 nm and the actual thickness was not determined. The contact resistance between the Z-2 NW and the Pt electrodes was ∼60 (500) kΩ at 300 (3) K, corresponding to a low specific contact resistivity of $1.8 \times 10^{-5}$ ($1.5 \times 10^{-4}$) Ω cm$^2$ at 300 (3) K. The contact resistances were somewhat larger in the Z-1 and Z-3 NWs. An SEM image for the representative four-probe Z-1 NW device is shown in figure 1(b).

Four-probe DC measurements had been carried out, utilizing a Keithley 2635A Sourcemeter as a current source as

well as a high-impedance voltmeter. The NW devices were placed on a sample holder which was situated inside a dark vacuum can. The vacuum can was mounted on a standard $^4$He cryostat. It should be noted that the resistances reported in this work were all measured by scanning the current–voltage ($I$–$V$) curves at various fixed temperatures between 1.3 and 320 K. The resistance at a given temperature was then determined from the regime around the zero bias voltage, where the $I$–$V$ curve was *linear*. Since we had employed the four-probe measurement configuration, the measured resistivities were thus the intrinsic resistivities of the individual NWs (and, obviously, should be independent of how the ohmic contacting electrodes were made). We mention in passing that the electrical resistivity of a single ZnO NW contacted by FIB-deposited Pt had recently been studied with varying lengths at room temperature, but the charge transport mechanisms were not addressed [14].

## 3. Results and discussion

Figure 1(a) shows our measured resistivities $\rho(T)$ as a function of reciprocal temperature for three individual ZnO NWs between 1.3 and 320 K. Figure 1(c) plots the $I$–$V$ curves for the Z-3 NW at five different measurement temperatures, as indicated in the caption to figure 1. Notice that the $I$–$V$ curves are linear (around zero bias). Figure 1(a) demonstrates that the resistivities increase monotonically with decreasing temperature, as would be expected for semiconductors. At our lowest measurement temperatures, the resistivity becomes essentially independent of temperature in every NW, indicating metallic-like conduction behavior [15]. Such degenerate behavior persists up to a higher temperature (a few degrees kelvin) in a more conductive NW. This observation immediately implies that these three NWs must lie close to the metal–insulator transition. Indeed, as has been previously established for single-crystalline ZnO materials and NWs, the values of room temperature resistivity $\rho(300\ \mathrm{K}) \approx 0.03$–$0.05\ \Omega$ cm (see table 1) would suggest values for charge carrier (donor) concentration, $n$, in the range $\approx 1 \times 10^{18}$ cm$^{-3}$ in these NWs [11, 16]. It is worth noting that this estimate is in good consistency with the concentration determined from the Hall effect measurement on a high-quality, epitaxially grown, unintentionally doped ZnO film [17], where $\rho(300\ \mathrm{K}) = 0.014\ \Omega$ cm and $n(1.7\ \mathrm{K}) = 3.2 \times 10^{18}$ cm$^{-3}$. In particular, recent time-resolved terahertz spectroscopy studies [18] have determined a carrier concentration of $\approx 1.9 \times 10^{18}$ cm$^{-3}$ for single-crystalline ZnO nanowires having a $\rho(300\ \mathrm{K}) \approx 0.016\ \Omega$ cm. For reference, the critical carrier concentration for the metal–insulator transition in ZnO is evaluated to be $n_c \simeq 5 \times 10^{18}$ cm$^{-3}$ [11, 19][4].

Compared with our previous samples studied in (I), the NWs investigated in the present work possess slightly lower resistivities and lie slightly closer to the metal–insulator transition. The difference in resistivities (or native doping concentrations) in these two sets of samples could easily be ascribed to different NW synthesis methods and growth conditions.

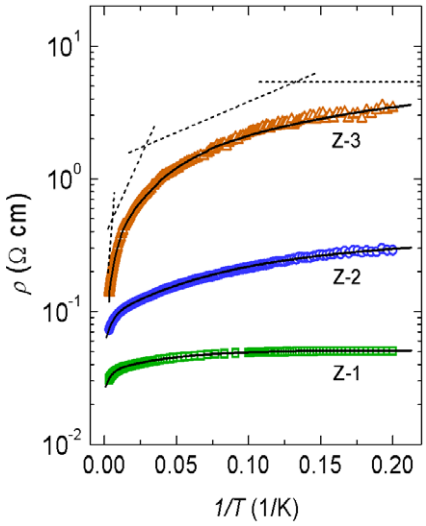


**Figure 2.** Variation of the logarithm of resistivity with reciprocal temperature for three ZnO NWs between 5 and 320 K. The solid curves are least-squares fits to equation (1) with the values of the fitting parameters listed in table 1. Notice that the theoretical predictions well describe the experimental data. The four straight dashed lines indicate the four contributions given by equation (1) for the Z-3 NW. For clarity, the resistivity of the Z-2 (Z-3) NW has been vertically shifted up by multiplying a factor of 2 (3).

Figure 2 shows the variation of the logarithm of resistivity with reciprocal temperature for the three NWs between 5 and 320 K. Here we want to concentrate on temperatures above 5 K so as to illustrate the *smooth* increase in $\rho$ with decreasing temperature, i.e. there is *no* visible straight regime in *any* temperature intervals in the log $\rho$–$(1/T)$ plot from 320 down to 5 K. (Note the large difference in the scales of abscissas between figures 1(a) and 2.) As proposed and explained in (I), the intrinsic resistivities in ZnO NWs are determined by a combination of the thermal activation conduction and the NNH conduction processes. The overall temperature behavior is given by [9, 11, 21]

$$\rho^{-1}(T) = \rho_1^{-1}\,\mathrm{e}^{-E_1/k_\mathrm{B}T} + \rho_2^{-1}\,\mathrm{e}^{-E_2/k_\mathrm{B}T} + \rho_3^{-1}\,\mathrm{e}^{-E_3/k_\mathrm{B}T} + \rho_0^{-1}, \quad (1)$$

where $\rho_i$ ($i = 1, 2, 3$) are temperature-independent resistivity parameters and $E_i$ are thermal activation energies describing the electronic conduction in the high ($E_1$), intermediate ($E_2$) and low ($E_3$) temperature regimes. The parameter $E_1$ represents the thermal activation energy of the electron from the Fermi level $\mu_\mathrm{F}$ to the conduction band, $E_2$ represents the thermal activation energy from $\mu_\mathrm{F}$ to the upper impurity ($\mathrm{D}^-$) band and $E_3$ represents the NNH conduction in the lower impurity (D) band. Inspection of figure 2 demonstrates that the theoretical predictions (solid curves) of equation (1) can well describe our experimental data (the symbols). In every NW, our least-squares-fitted values, which are listed in table 1, satisfy the conditions $E_1 > E_2 > E_3$ and $\rho_1 < \rho_2 < \rho_3$, as required for equation (1) to be applicable [11].

[4] The values of critical carrier concentration $n_c$ predicted for the Mott-type and the Anderson-type metal–insulator transitions are similar [20]. In ZnO NWs, the nature of the metal–insulator transition deserves further studies and clarifications.

Theoretically, it is known that the $E_2$-conduction process can only happen for a bounded range of dopant concentration not far below $n_c$ [9, 11, 21]. This prerequisite is consistent with our estimate of the carrier concentration ($\approx 1 \times 10^{18}$ cm$^{-3}$, which is not much below $n_c$) in our NWs mentioned above. Notice that, in equation (1), we have added a temperature-independent term $\rho_0^{-1}$ to account for the constant ('parallel') conductivity due to the degenerate behavior occurring at very low temperatures[5]. As for illustrations, the four straight dashed lines in figure 2 indicate the four contributions given by equation (1) for the representative Z-3 NW. It is seen that the $E_1$-, $E_2$- and $E_3$-conduction channels roughly dominate at temperatures in the regime of ~180–320 K, ~35–180 K and ~7–35 K, respectively.

Our fitted values of $E_1$ listed in table 1 are very acceptable. The activation energies of $\simeq$23–26 meV correspond to the major shallow donor levels in natively doped ZnO materials, which could be due to Zn interstitials, oxygen vacancies or hydrogen impurities[6]. These experimental values fall at the lower end of the typical $E_1$ values (~20–45 meV) found in many ZnO materials and NWs [1, 8, 11], because the three NWs lie quite close to the metal–insulator transition. In addition, our fitted values of $E_2$ (~2–5 meV) and $E_3$ ($\lesssim$1 meV) are in line with the corresponding values reported in (I). Notice that the value of $E_3$ in the Z-1 NW is essentially zero, because this particular NW possesses the lowest resistivity among our samples (including those NWs studied in (I)). Theoretically, it is expected that $E_3 \rightarrow 0$ as the sample approaches the metal–insulator transition [21]. Thus, equation (1) faithfully describes the *intrinsic* electrical conduction processes in single-crystalline, natively doped ZnO NWs. Pertinent optical experiments specifically designed to probe the features of the upper impurity $D^{-1}$ band would be of great interest and could further substantiate the validity of equation (1) [22].

Let us now comment on the physical explanation for the charge conduction processes in natively doped ZnO NW materials.

(1) We point out that our measured $\rho(T)$ in the Z-2 and Z-3 NWs cannot be fitted with only two conduction channels, for example, by ignoring the second term and setting $\rho_2^{-1} = 0$ in equation (1). (This would have been the case if the impurity band did not split into two subbands [9, 15].) In the Z-1 NW, the NNH ($E_3$) conduction term becomes nominally temperature-independent and, in practice, cannot be separated from the constant ($\rho_0^{-1}$) term. Therefore, the measured $\rho(T)$ can alternatively be fitted to equation (1) by ignoring the $\rho_3$ term. In this case, the fitted values of $\rho_1$, $\rho_2$, $E_1$ and $E_2$ are basically unchanged (see table 1), as expected.

(2) We emphasize that the overall temperature behavior of our measured $\rho(T)$ in every NW cannot be consistently described by a contribution from either the Mott VRH conduction ($\rho \propto \exp(T_0/T)^{1/4}$, where $T_0$ is a characteristic temperature) [7] or the Efros–Shklovskii VRH conduction ($\rho \propto \exp(T_0^*/T)^{1/2}$, where $T_0^*$ is a characteristic temperature) [9] process. On the other hand, to fully unravel the charge conduction processes, it should be of great interest to investigate highly resistive ZnO NWs deep on the semiconducting side and in the absence of a degenerate channel. In that case, a crossover from the NNH ($E_3$) conduction to the VRH conduction processes might take place at very low temperatures.

(3) By accepting equation (1), one may reason that the effect of the diverging electrical quantities ($\rho$, $n$, etc) [4] found in different ZnO NWs grown by various groups is mainly to modify the subtle details of the split impurity band structure. Such subtle modifications will then lead to slightly differing values of the activation energies $E_i$s (and also the resistivity parameters $\rho_i$s). More precisely, the values of $E_i$s are expected to vary among as-grown NWs in a predictable manner, depending basically on how close the NWs fall to the metal–insulator transition, but largely independent of which particular method they are synthesized by. In short, we think that the seemingly diverging electrical quantities reported in the literature should not imply that there exist any differing conduction mechanisms in natively doped ZnO NWs[7].

(4) As has been discussed in (I), for ZnO NWs on the semiconducting side, the electrical transport is through the 'bulk' of the NW. On the other hand, for ZnO NWs on the metallic side, a surface conduction channel has recently been experimentally observed from two-dimensional weak-localization magnetoresistance [11] and resistance [6] measurements. How the bulk degenerate ($\rho_0^{-1}$) term on the semiconducting side gradually develops into (or emerges with) the surface conduction channel on the metallic side deserves further experimental clarifications. For instance, in addition to studying the two-dimensional weak-localization and electron–electron interaction effects [23], examining possible Aharonov–Bohm-like oscillations [24] (or, more precisely, the Altshuler–Aronov–Spivak (AAS) oscillations [25]) in the presence of parallel magnetic fields along the NW axis could provide useful information.

## 4. Conclusion

We have measured the intrinsic resistivities between 1.3 and 320 K in three natively doped ZnO NWs synthesized via carbon thermal chemical vapor deposition. The overall temperature behavior of $\rho(T)$ can be well described by a combination of the thermal activation conduction and the nearest-neighbor hopping conduction processes. The magnitudes of the extracted activation energies are consistent with the known physical picture. This study, taken together

[5] The finite value of $\rho_0^{-1}$ suggests the presence of a temperature-independent (or an extremely weakly temperature-dependent) metallic-like conduction channel as $T \rightarrow 0$ K. This channel becomes progressively more pronounced in the samples lying closer to the metal–insulator transition. In the investigation of the charge conduction mechanisms in semiconducting ZnO NWs, we are more interested in the temperature-dependent conduction processes, i.e. the first three terms in equation (1).

[6] The identification of the microscopic origins of the major shallow donors and their associated energy levels in ZnO is still under intense theoretical and experimental investigations. See, for recent reviews, [2] and [3].

[7] However, as mentioned in section 1, in the two-probe measurements the contact resistances will cause extra and, sometimes, misleading complications.

with our previous work (I) which employed a different sample growth method as well as a different electron-beam lithography electrode technique, strongly demonstrates that the electrical conduction processes in ZnO NWs are predictable and now satisfactorily understood.

Finally, we would like to stress that, unlike polycrystalline ZnO films, single-crystalline ZnO NWs are free of grain boundaries and thus they provide a model system for the studies of the intrinsic electrical conduction processes in this scientifically and technologically alluring material, without any complications from, for example, the thermionic emission effect [26].

## Acknowledgments

This work was supported by the Taiwan National Science Council through grant no. NSC 98-2120-M-009-004 and by the MOE ATU Program (JJL). Research by JGL was supported by NSF.

## References

[1] Ozgür Ü, Alivov Ya I, Liu C, Teke A, Reshchikov M A, Doğan S, Avrutin V, Cho S J and Morkoç H 2005 *J. Appl. Phys.* **98** 041301
[2] Janotti A and Van de Walle C G 2009 *Rep. Prog. Phys.* **72** 126501
[3] McCluskey M D and Jokela S J 2009 *J. Appl. Phys.* **106** 071101
[4] Schlenker E, Bakin A, Weimann T, Hinze P, Weber D H, Gölzhäuser A, Wehmann H H and Waag A 2008 *Nanotechnology* **19** 365707
[5] Heo Y W, Tien L C, Norton D P, Kang B S, Ren F, Gila B P and Pearton S J 2004 *Appl. Phys. Lett.* **85** 2002
[6] Hu Y, Liu Y, Li W, Gao M, Liang X, Li Q and Peng L M 2009 *Adv. Funct. Mater.* **19** 2380
[7] Mott N F and Davis E A 1979 *Electronic Processes in Non-Crystalline Materials* (Oxford: Clarendon)
[8] Chang P C and Lu J G 2008 *Appl. Phys. Lett.* **92** 212113
[9] Shklovskii B I and Efros A L 1984 *Electronic Properties of Doped Semiconductors* (New York: Springer)
[10] Ma Y J, Zhang Z, Zhou F, Lu L, Jin A and Gu C 2005 *Nanotechnology* **16** 746
[11] Chiu S P, Lin Y H and Lin J J 2009 *Nanotechnology* **20** 015203
[12] Lin Y F, Jian W B, Wang C P, Suen Y W, Wu Z Y, Chen F R, Kai J J and Lin J J 2007 *Appl. Phys. Lett.* **90** 223117
[13] Chang P C, Chien C J, Stichtenoth D, Ronning C and Lu J G 2007 *Appl. Phys. Lett.* **90** 113101
[14] He J H, Chang P H, Chen C Y and Tsai K T 2009 *Nanotechnology* **20** 135701
[15] Mott N F and Twose W D 1961 *Adv. Phys.* **10** 107
[16] Ellmer K 2001 *J. Phys. D: Appl. Phys.* **34** 3097
[17] Reuss F, Frank S, Kirchner C, Kling R, Gruber Th and Waag A 2005 *Appl. Phys. Lett.* **87** 112104
[18] Baxter J B and Schmuttenmaer C A 2006 *J. Phys. Chem.* B **110** 25229
[19] Tampo H, Yamada A, Fons P, Shibata H, Matsubara K, Iwata K, Niki S, Nakahara K and Takasu H 2004 *Appl. Phys. Lett.* **84** 4412
[20] Mott N F 1993 *Conduction in Non-Crystalline Materials* (Oxford: Clarendon)
[21] Mott N F and Davis E A 1968 *Phil. Mag.* **17** 1269
[22] Norton P 1976 *Phys. Rev. Lett.* **37** 164
[23] Lin J J and Giordano N 1987 *Phys. Rev.* B **35** 545
[24] Washburn S and Webb R A 1986 *Adv. Phys.* **35** 375
[25] Altshuler B L, Aronov A G and Spivak B Z 1981 *JETP Lett.* **33** 94
[26] Tsurumi T, Nishizawa S, Ohashi N and Ohgaki T 1999 *Japan. J. Appl. Phys.* **38** 3682